Nanoscale

PAPER

View Article Online
View Journal | View Issue

Cite this: *Nanoscale*, 2016, **8**, 19744

# A self-quenching-resistant carbon nanodot powder with multicolored solid-state fluorescence for ultra-fast staining of various representative bacterial species within one minute†

Yongqiang Zhang,‡[a,b] Chunfeng Li,‡[c,d,e] Yi Fan,*[a] Chengbin Wang,[d] Ruifu Yang,[c] Xingyuan Liu*[a] and Lei Zhou*[c]

Received 18th August 2016,
Accepted 1st November 2016

DOI: 10.1039/c6nr06553h

www.rsc.org/nanoscale

In this study, we prepared self-quenching-resistant solid-state fluorescent carbon nanodots (SFCDs) without any other solid matrices. The SFCDs were prepared using a one-step microwave synthesis method through precise control of the heating power and time. The resulting SFCD powder showed excitation-dependent emission behavior with a maximum fluorescence quantum yield of 40%. The multicolored SFCDs were successfully used as fluorescent agents for rapid staining of 14 representative bacterial species, including Gram-negative, Gram-positive, and acid-fast bacteria. Moreover, some pathogenic bacteria, including *Bacillus anthracis* (vegetative cells and endospores), *Yersinia pestis*, *Vibrio cholera* O1, *Listeria monocytogenes*, *Neisseria meningitidis*, and *Klebsiella pneumoniae*, could all be stained within just 1 min by the smear staining method without any incubation, which was also applicable by using the liquid incubation method. Moreover, excellent staining quality, superior resistance to photobleaching, high stability in solutions of different pH values, and low toxicity were also demonstrated.

## Introduction

As a new type of carbon-based nanomaterial, carbon nanodots (CDs) have recently gained great interest in bioimaging, photocatalysis, sensors, lasers, light-emitting diodes (LEDs), and photovoltaic devices because of their simple preparation, low toxicity, good luminescence properties, stability, and excellent biocompatibility in comparison with organic dyes and other semiconductor quantum dots with heavy metal cores.[1] However, CDs suffer from aggregation-induced quenching (AIQ), which leads to quenching of fluorescence in the solid state or when CDs are used at high concentrations.[2] AIQ limits the wide application of CDs. For example, optoelectronic devices and lasers generally require luminescent materials emitting in the solid state;[1c–e] however, to date, almost all CD-related research has concentrated on the fluorescence of CDs in aqueous solution. Such studies are insufficient for supporting and expanding the applications of these nanomaterials.[2b]

Microbial contamination of food is a major food safety problem worldwide. Total bacterial count (TBC) is one of the

[a]*State Key Laboratory of Luminescence and Applications, Changchun Institute of Optics, Fine Mechanics and Physics, Chinese Academy of Sciences, Changchun 130033, China. E-mail: fanyi@ciomp.ac.cn, liuxy@ciomp.ac.cn*
[b]*University of Chinese Academy of Sciences, Beijing 100049, China*
[c]*Laboratory of Analytical Microbiology, State Key Laboratory of Pathogen and Biosecurity, Beijing Institute of Microbiology and Epidemiology, Beijing 100071, China. E-mail: ammszhoulei@aliyun.com*
[d]*Department of Clinical Laboratory, Chinese People's Liberation Army General Hospital, Beijing 100853, China*
[e]*Department of Blood Transfusion, The Second Hospital of Shandong University, Jinan 250033, China*

† Electronic supplementary information (ESI) available: Fig. S1: The process procedures in microwave synthesis of SFCDs and SNCDs; Table S1: Surface functional groups of SFCDs identified by FT-IR spectra; Fig. S2: The full scan XPS spectra of SFCDs and SNCDs; Table S2: Lifetimes of SFCDs and SNCDs; Fig. S3: Absorption and PL spectra of SNCD powder; Table S3: Comparisons between SFCDs and SNCDs; Fig. S4: Fluorescence intensities and PL decay curves of SFCD solutions with different concentrations; Fig. S5: Fluorescence intensities and PL decay curves of SNCD solutions with different concentrations; Fig. S6: Fluorescence stability of SFCDs on a stained smear and under lucifuge storage; Fig. S7: Confocal fluorescence microscopy images of SFCD-stained bacteria; Table S4: Comparisons of our work with other 12 previous studies; Fig. S8: A comparison of the staining effect on *Bacillus anthracis* endospores using the 1 min-SFCD-SSM and 1 min-SFCD-LIM; Fig. S9: A comparison of the staining effect on intact *Escherichia coli* cells and *Escherichia coli* cell debris; Fig. S10: One minute staining effect of *Staphylococcus aureus* bacteria samples on the dependence of concentration of SFCD solution; Fig. S11: Graph of one minute effect of *Staphylococcus aureus* bacteria samples on the dependence of concentration of SFCD solution; Fig. S12: The PL excitation (PLE) and PL spectra of SFCD solution (100 mg $mL^{-1}$); Fig. S13: The lay scanning images of a HeLa cell; Fig. S14: The lay scanning images of an *Escherichia coli* cell; Fig. S15: The magnification image of an *Escherichia coli* cell; Video S1: Three-dimensional video of an *E. coli* cell. See DOI: 10.1039/c6nr06553h

‡ These authors contributed equally to this work.

most important pollution indexes for evaluating food quality and is therefore an important parameter in quality control. Indeed, the real-time monitoring of pathogenic bacteria plays a key role in microbiology, environmental protection, clinical diagnostics, customs examination, and food safety.[3] Staining-based bioimaging that can make microbes visible and countable is a powerful tool for real-time identification of bacterial contamination. CDs are promising candidates for bioimaging agents; however, the ability of CDs to stain bacteria with diverse structures, particularly those with complex shells (containing a cell membrane, cell wall, and even capsule), is unclear, and most bacteria reported to be stained by CDs to date have been strains of *Escherichia coli* and *Staphylococcus aureus*.[4] Moreover, the staining process requires incubation for 12 to 24 h,[4a–c] which is not feasible for real-time monitoring. Additionally, the bioimaging applications of CDs are limited by AIQ, which leads to nonuniform staining and weak fluorescence images.[1i,k,5] Accordingly, synthesis of CDs that can stain various species of bacteria in real-time and effectively without concentration-dependent fluorescence quenching is needed. Solid-state fluorescent CDs (SFCDs) have been fabricated to resist AIQ by dispersion in solid matrices, such as polyvinyl pyrrolidone (PVP),[6] polyacrylamide (PAM),[6] polyacrylic acid (PAA),[6] polyvinyl alcohol (PVA),[7] polyethyleneglycol (PEG),[8] polymethylmethacrylate (PMMA),[9] starch,[10] and silica xerogel.[11] Chen *et al.* reported a type of self-quenching-resistant CD powder using PVA and ethylenediamine as a precursor; the resulting CDs exhibited a fluorescence quantum yield (FQY) of 35%.[2a] Yang and coworkers demonstrated that PEG-functionalized CDs have weak staining capability due to the resistance of PEG to protein and reduced interactions between the CDs and biological cells.[12] In our opinion, solid-state fluorescent CDs with solid matrices, added during or after the synthesis, may diminish the bio-affinity interactions between CDs and biological cells and reduce the biocompatibility of the materials. Xu and coworkers reported a type of solid state CDs using calcium citrate and urea as raw materials prepared through microwave synthesis; the FQY of the CDs in solvents was 10%, whereas that of the CDs in solid state was not described.[13] These solid-state fluorescent CDs all lack application in bioimaging. Therefore, FQY SFCDs without any other solid matrices are needed for bioimaging applications.

Here we report simple, low-cost, self-quenching-resistant, solid-state fluorescent CDs (SFCDs) without any solid matrices and their application in the imaging of 14 representative bacterial species to significantly improve rapid detection using TBC technology. The SFCDs exhibited a high FQY of 40%, with the strongest peak at 458 nm; to the best of our knowledge, this is the highest FQY reported for SFCDs in solid-state emitting in the blue light region without any other solid matrices. In our work, fluorescence images under a laser-scanning confocal microscope (LSCM) showed that typical bacteria, including seven species of Gram-negative bacteria, six species of Gram-positive bacteria, and one species of acid-fast bacteria, *i.e.*, *Bacillus anthracis* (vegetative cells and endospores), *Bacillus subtilis* (vegetative cells and endospores), *Clostridium sporogenes* (vegetative cells and endospores), *Listeria monocytogenes*, *Enterococcus faecalis*, *Staphylococcus aureus*, *Streptococcus pneumoniae*, *Yersinia pestis*, *Vibrio cholera* O1, *Neisseria meningitidis*, *Klebsiella pneumoniae*, *Pseudomonas aeruginosa*, *Escherichia coli*, and *Mycobacterium smegmatis*, could be detected. In particular, this stain detected *Bacillus anthracis* endospores (with thick capsules),[14] *Neisseria meningitidis* and *Klebsiella pneumoniae* (with lipids and polysaccharides contained in their cell walls),[15] and *Mycobacterium smegmatis* (with large amounts of lipids contained in its cell walls),[16] which are usually difficult to stain because of their cell wall compositions or the extremely robust structure of their thick capsules. Staining of these bacteria was achieved within 1 min, without any incubation, and the fluorescence images were bright, had clear contours, and exhibited no interference from other biological impurities. In addition to their excellent staining quality, superior resistance to photobleaching, good stability in solutions of different pH values, and low toxicity were also demonstrated.

## Materials and methods

### Materials

Urea and citric acid were purchased from Sinopharm Chemical Reagent Co., Ltd, (Shanghai, China). Peptone, agar powder, yeast extract powder, $Ca(NO_3)_2$, $MgSO_4$, $FeSO_4$, KCl, $MnCl_2$, NaCl, and $Na_3N$ were all purchased from Sigma-Aldrich (St Louis, MO, USA). Dried meat particle and cooked meat medium base were obtained from Beijing Land Bridge Technology Co., Ltd (Beijing, China). The LIVE/DEAD® *Bac*Light™ Bacterial Viability and Counting Kit (with SYTO® 9 dye and propidium iodide contained in the kit) and foetal bovine serum (FBS) were purchased from Life Technologies (Carlsbad, CA, USA). Dulbecco's modified Eagle's medium (DMEM) was purchased from Neuronbc Co., Ltd (Beijing, China), and 0.25% trypsin from Bioscience Co., Ltd (Dümmer, Germany). All chemical reagents were of analytical grade with no further purification, and supplied by Sinopharm Chemical Reagent Co., Ltd (Shanghai, China). The water used in all experiments was purified with a Millipore system.

### Synthesis of SFCDs

Two grams of urea and 3.5 g of citric acid were added to 10 mL deionized water, which was subjected to ultrasonic treatment. The solution was heated with a stationary heating curve in a power-tunable microwave oven (Fig. S1a†). The whole reaction was carried out in 3 min. There were five sections of continuous heating; the first and second processes functioned to quickly dry the water, with the second process having a lower power and an intermediate interval to avoid bumping. The water was almost completely removed after the first two heating steps, and the next heating step was the crucial reaction for dehydration. The remaining heating steps functioned in further carbonization of the unreacted polymeric structures. Stirring and shaking were necessary during these intervals to ensure that the components reacted evenly, and the heating power was gradually reduced to prevent rapid warming, which

could induce excessive carbonization. Finally, the solution changed into a viscous gel with a light yellow color. It became solid after cooling to room temperature, and the solid was then ground into a powder, washed with acetone, and centrifuged (10 000 rpm [6640.6*g*], 10 min) twice to wash off residual raw materials. The precipitate was dissolved in deionized water and centrifuged at 10 000 rpm for 10 min to remove agglomerated or large particles. Then, the supernatant was further purified using a 0.02 μm filter (GE Whatman, Anotop). After this procedure, the solution was freeze-dried to a powder and collected.

### Synthesis of solid-state non-fluorescent CDs (SNCDs)

Two grams of urea and 3.5 g of citric acid were added to 10 mL deionized water, which was treated by ultrasonication. The solution was transferred to a power-tunable microwave oven and heated with a heating curve (the heating curve is shown in Fig. S1b†) using a process similar to that used for the synthesis of SFCDs, but with the same power for the three terminal heating sections. After reaction, the purification was carried out as described for the synthesis of SFCDs.

### Preparation of SFCD and SNCD staining solutions

The resulting SFCDs were dissolved in saline solution to form a staining solution at a certain concentration.

The SNCD staining solution was prepared with SNCDs using the same methods as used for SFCDs.

### Bacterial cultures

The representative Gram-positive bacteria were *Streptococcus pneumoniae*, *S. aureus*, *Enterococcus faecalis*, *B. anthracis* (vegetative cells and endospores), *Bacillus subtilis* (vegetative cells and endospores), *C. sporogenes* (vegetative cells and endospores), and *Listeria monocytogenes*. The representative Gram-negative bacteria were *N. meningitidis*, *Pseudomonas aeruginosa*, *Yersinia pestis*, *Vibrio cholera* O1, *K. pneumoniae*, and *E. coli*. Additionally, the acid-fast bacterium like *M. smegmatis*, and the mammalian cell like HeLa were also used in this work.

The mammalian and bacteria cells were cultured in commonly used medium with traditional methods up to the logarithmic phase. For endospore preparation, *B. subtilis* and *B. anthracis* were grown on nutrient agar plates (containing 3 g $L^{-1}$ yeast extract powder, 6 g $L^{-1}$ tryptone, 1 g $L^{-1}$ KCl, 10 g $L^{-1}$ NaCl, 0.122 g $L^{-1}$ $MgSO_4$, 0.23 g $L^{-1}$ $Ca(NO_3)_2$, 0.0002 g $L^{-1}$ $FeSO_4$, 0.197 g $L^{-1}$ $MnCl_2$, and 15 g $L^{-1}$ agar powder) at 37 °C for 7 d. The vegetative cells were put in sterilized distilled water and lysed by osmotic pressure, and the resultant endospores were 99% pure as determined by microscopy observation. For endospore formation, *C. sporogenes* were grown in cooked meat medium under anaerobic conditions at 37 °C for 3 days. Pure cultures were collected using centrifugation at 7000 rpm for 15 min. The resultant pellet was washed three times by resuspension and centrifugation in sterilized saline. The population was determined *via* a Luria-Bertani (LB) agar plate count.

The pure culture of HeLa cells was treated with 0.25% trypsin to facilitate cell suspension. Whole *E. coli* cells were subjected to ultrasonication to prepare cell debris.

### Bacterial and cell staining

Fourteen representative species of all bacteria (including endospores) were stained with SFCDs by the smear staining method (SSM). For the 1 min-SFCD-SSM, bacterial suspensions (vegetative cell or endospore) with a concentration of ~$10^8$ cfu $mL^{-1}$, *E. coli* cell debris, or HeLa cell suspensions were smeared onto a glass slide to form a thin layer of cells. The slide was air dried and passed over a flame two or three times to fix the cells (to avoid centrifugation-based separation of bacterial cells and SFCDs which helps to control staining time accurately and maintain cell integrity). Subsequently, the slide was covered with SFCDs in saline solution at an optimized concentration of 100 mg $mL^{-1}$ to ensure that all bacteria were covered. After they were kept standing for one minute at room temperature, the residual SFCDs were washed out for 5 sec with deionized water. The *B. anthracis* endospore was also stained with SFCDs for one minute using the liquid incubation method (LIM); for the 1 min-SFCD-LIM, *B. anthracis* endospores with a concentration of ~$10^8$ cfu $mL^{-1}$ were incubated with 100 mg $mL^{-1}$ SFCDs saline solution for one minute (accepted liquid incubation methods, excluding the time for centrifugation-based separation). Cells were then separated by centrifugation and rinsed with buffer before the stained endospores were fixed on a slide.

According to the manufacturer's instructions, SYTO9 dye was diluted to a standard working concentration of $5.07 \times 10^{-6}$ mol $L^{-1}$. Then a standard staining operation (namely a 15 min-SYTO9-LIM, in which the mixture of bacterial suspension and SYTO9 was incubated for 15 min at room temperature, the cells were separated and rinsed by centrifugation, and the stained cells fixed onto a slide) and a rapid staining operation (namely the 1 min-SYTO9-SSM, which was similar to the 1 min-SFCD-SSM) were carried out. After natural drying of the slides, we dropped the mounting medium (glycerol : saline (9 : 1) solution) onto them and they were stamped. The stained slides were examined with the same parameters under oil immersion (630×) on an Olympus FV1000 LSCM. All of the bacterial experiments were performed at State Key Laboratory of Pathogen and Biosecurity by strictly following the related safety operation rules.

### Characterization

High-resolution transmission electron microscopy (HRTEM) images and fast Fourier transform (FFT) spot diagrams were taken with a FEI-TECNAI G2 transmission electron microscope operating at 200 kV. The TEM sample was prepared by depositing a drop of dilute SFCD aqueous solution on a carbon-coated copper grid. X-ray photoelectron spectroscopy (XPS) was determined by using a Thermo Scientific ESCALAB 250 for multitechnique surface analysis. A Bio-Rad Excalibur FTS 3000 spectrometer with KBr tablets was used to measure the Fourier transform infrared (FTIR) spectra of SFCDs. A F-7000 Hitachi Fluorescence Spectrometer was used to detected photoluminescence excitation (PLE) and photoluminescence (PL) emission spectra. Fluorescence lifetimes and absolute fluorescence quantum yield were determined by using an Edinburgh

 

FLS920 spectrometer equipped with a calibrated integrating sphere. A Shimadzu UV-3101 spectrophotometer is used in the measurement of ultraviolet/visible (UV/Vis) absorption (ABS) spectra. Confocal fluorescence microscopy images were obtained by using an Olympus FV1000 confocal laser microscope.

## Results and discussion

TEM was used for characterization of the morphology of the synthesized SFCDs and SNCDs. TEM images illustrated that the SFCDs and SNCDs were torispherical nanoparticles with different average diameters of 2.3 and 5.8 nm, respectively; the SFCDs exhibited a narrow size distribution range of 1–5 nm, whereas that of the SNCDs was more broad (3–11 nm; Fig. 1a and b). HRTEM images revealed a lattice spacing distance of 3.2 Å, which corresponded to the (002) graphite facet.[17] The SFCD and SNCD compositions were determined by FTIR spectra. As is shown in Fig. 1c and Table S1,† the broad absorption band at 3400 $cm^{-1}$ was assigned to the stretching vibrations of O–H and N–H, the strong peaks of 1720 and 1670 $cm^{-1}$ were attributed to the vibrational absorption band of C=O in the carboxylate and carboxyl groups, respectively, while the peaks at 1350 and 1208 $cm^{-1}$ were observed due to the two bending vibrations of C–O–C.[18] The SNCDs showed weaker absorption bands for –OH and C=O in the carboxyl group and stronger peak intensities for C–O–C bonds and C=O in the carboxylate group; we assumed that these observations could be explained by the abundant carboxylic ester groups, which originated from further dehydrate condensation between –OH and –COOH. These compositions were also confirmed by XPS. Full scans by XPS showed the presence of O 1s, C 1s, and N 1s with peaks located at 531, 284, and 400 eV, respectively (Fig. S2†).[1b] High-resolution C 1s spectra showed the existence of graphene $sp^2$ C at 284.6 eV and $sp^3$ C at 288.5, 286.7, and 285.7 eV in the C=O, C–O, and C–N groups, respectively (Fig. 1d).[1b] The high-resolution N 1s spectra revealed two different types of nitrogen doping: pyrrolic nitrogen at about 398.2–399.5 eV, and graphitic nitrogen at about 400.5–401.5 eV (Fig. 1e).[19] The high-resolution O 1s spectra showed the existence of C–O–C at 533.0 eV and C=O at 531.6 eV (Fig. 1f).[1b] We further determined the amounts of the different types of chemical bonds for SFCDs and SNCDs (see Table 1); in comparison with the SFCDs, SNCDs possessed larger amounts of C=O and C–O–C bonds, consistent with FTIR spectroscopy analysis. Additionally, the stronger graphitic-N was attributed to the transformation from pyrrolic nitrogen and the deeper extent of N-doping.[19a,20]

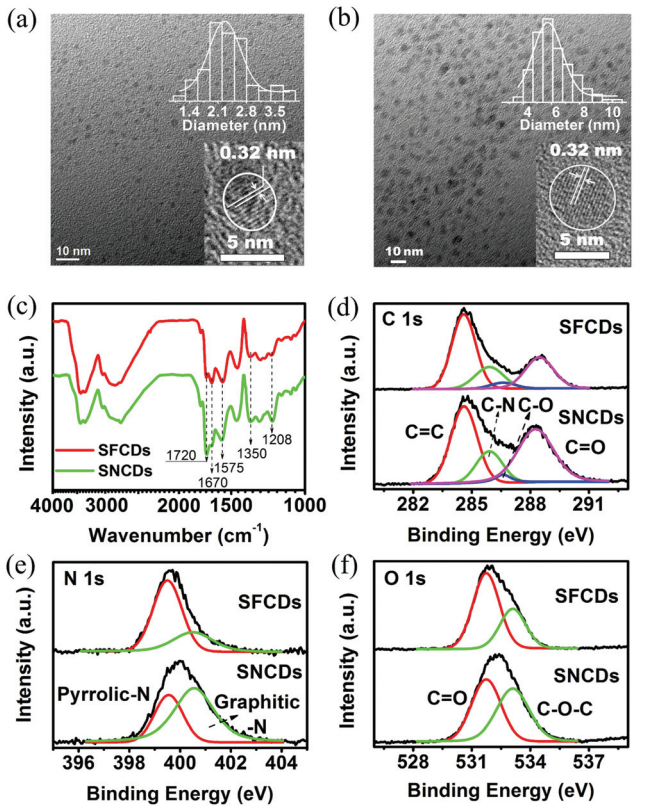


**Fig. 1** Morphology and chemical structure characterization of SFCDs and SNCDs. (a) Transmission electron microscopy (TEM) image of SFCDs; (b) TEM image of SNCDs (upper inset: size distribution, lower inset: HRTEM image). (c) FTIR spectra of SFCDs (red line) and SNCDs (green line). (d) High-resolution C 1s spectra of SFCDs and SNCDs. (e) High-resolution N 1s spectra of SFCDs and SNCDs. (f) High-resolution N 1s spectra of SFCDs and SNCDs.

Photographs of SFCD and SNCD powders were taken under daylight conditions and a UV-lamp (Fig. 2a and b). A bright fluorescence of the SFCD powder was observed under the UV-lamp, whereas no obvious fluorescence was observed for the SNCD powder due to AIQ, as previously reported.[2b] The fluorescence emission behavior of the SFCD powder tablet samples was explored under different excitation wavelengths, as illustrated in Fig. 2c. The SFCDs exhibited tunable solid-state fluorescence. The absorption and PL spectra of the SFCD powder are shown in Fig. 2d. The SFCDs showed two absorption peaks at 240 and 336 nm; the former peak was assigned

**Table 1** The amounts of various chemical bonds in SFCDs and SNCDs, as determined by XPS spectra

| | C 1s | | | | N 1s | | O 1s | |
|---|---|---|---|---|---|---|---|---|
| Sample | C=C | C–N | C–O | C=O | Pyrrolic-N | Graphitic-N | C=O | C–O–C |
| SFCDs | 0.51 | 0.18 | 0.04 | 0.27 | 0.07 | 0.03 | 0.28 | 0.16 |
| SNCDs | 0.39 | 0.17 | 0.04 | 0.40 | 0.08 | 0.16 | 0.29 | 0.30 |

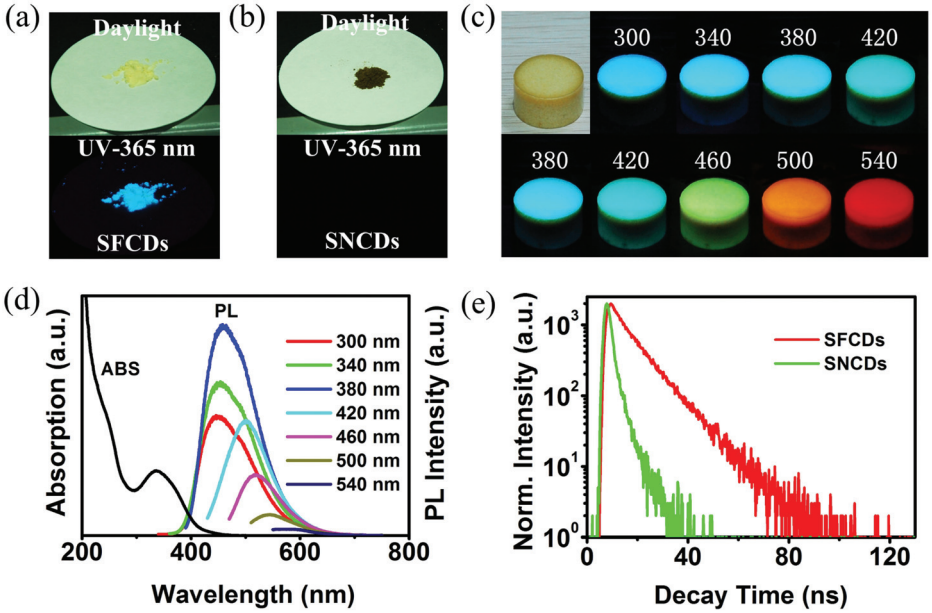


**Fig. 2** (a) Photographs of SFCD powder under daylight and a UV-lamp; (b) photographs of SNCD powder under daylight and a UV-lamp; (c) photographs of a SFCD tablet sample taken under normal daylight conditions and at various excitation wavelengths (indicated above the corresponding images). (d) Absorption (ABS) and PL spectra of SFCD powder in the excitation wavelength range of 300 to 540 nm. (e) PL decay curves for SFCD and SNCD powders.

to the $\pi \rightarrow \pi^*$ transitions, and the latter was assigned to the $n \rightarrow \pi^*$ transition.[21] The PL emission peak was red-shifted from 446 to 600 nm as the excitation wavelength varied from 300 to 540 nm (Fig. 2d). The strongest PL peak was located at 458 nm with a maximum FQY of 40% in the solid state. To the best of our knowledge, this is the highest FQY reported for solid state CDs in the blue light region without any other solid matrices. The absorption and PL spectra of the SNCD powder were also detected (Fig. S3†). The SNCD powder had very weak fluorescence, and the FQY of the SNCDs was found to be 1%. The PL decay curves of the SFCDs and SNCDs are shown in Fig. 2e and Table S2.† The lifetimes ($\tau_{avg}$) of the SFCDs and SNCDs were 9.11 and 1.42 ns, respectively. The radiative transition rate ($K_R$) and non-radiative transition rate ($K_{NR}$) could be obtained from $\tau$ and $\Phi$ using formulas (1) and (2):

$$\tau = (K_R + K_{NR})^{-1} \quad (1)$$

$$\Phi = K_R \cdot (K_R + K_{NR})^{-1} \quad (2)$$

where $\Phi$ is the FQY, and $\tau$ is the average lifetime. The $K_R$ and $K_{NR}$ of the SFCDs and SNCDs are shown in Table 2. The SNCDs exhibited a large $K_{NR}$ and a small $K_R$ in the solid state. In principle, the ratio of $K_R$ and $K_{NR}$ is the major determinant of FQY among fluorescent materials; the FQY is proportional to $K_R/K_{NR}$.[22] The resulting $K_R/K_{NR}$ ratios of the SFCD and SNCD powder were 0.67 and 0.01, respectively, which could explain the differences in solid-state fluorescence between the SFCDs and SNCDs. In addition, the fluorescence intensities and PL decay curves of SFCD solutions with different concentrations were measured. As shown in Fig. S4,† the fluorescence intensity of the SFCD solution showed slight changes (less than 0.1 of the initial intensity) as the concentration increased from 0.1 to 100 mg $mL^{-1}$. The lifetimes were measured to be 12.45, 12.42, 11.43, 10.28, and 9.11 ns at concentrations of 0.1, 1, 10, and 100 mg $mL^{-1}$ and in the solid state, respectively, demonstrating the occurrence of low energy transfer, similar to a previous report.[2a] These values were obviously different from those of common fluorescent materials showing high energy transfer and AIQ. In contrast, measurement of the fluorescence intensities and PL decay curves of SNCD solutions with different concentrations in Fig. S5† showed that the fluorescence was greatly quenched as the concentration increased owing to AIQ; the lifetimes were measured to be 8.64, 3.67, and 1.42 ns for the concentrations of 0.1 and 1 mg $mL^{-1}$ and for the solid state, respectively. Thus, the lifetime decreased substantially as the concentration increased, demonstrating the occurrence of energy transfer.[2a] More comparisons between SFCDs and SNCDs are shown in Table S3.†

**Table 2** The values of $\Phi$, $\tau_{avg}$, $K_R$, $K_{NR}$, and $K_R/K_{NR}$ in SFCDs and SNCDs

| Sample | $\Phi$ | $\tau_{avg}$ (ns) | $K_R$ ($s^{-1}$) | $K_{NR}$ ($s^{-1}$) | $K_R/K_{NR}$ |
|---|---|---|---|---|---|
| SFCDs | 40% | 9.11 | $4.39 \times 10^7$ | $6.59 \times 10^7$ | 0.67 |
| SNCDs | 1% | 1.42 | $7.04 \times 10^6$ | $6.97 \times 10^8$ | 0.01 |

Fluorescence images under LSCM were used to visualize bacteria cells with CD staining for fluorescence imaging. To compare the staining abilities of SFCDs and SNCDs, *Staphylococcus aureus* cells were stained with SSM for 1 min. Additionally, 15 min-SYTO9-LIM-staining (a standard

 

operation in SYTO9 staining) and 1 min-SYTO9-SSM-staining were carried out as control groups; the fluorescence images are shown in Fig. 3a. The SFCDs were perfectly dispersed in the *Staphylococcus aureus* cells. The images were bright and uniform with clear contours. The staining effects of the SNCDs were unsatisfactory; that is, the fluorescence images of 1 min-SNCD-SSM samples were faint and dim, potentially because of the larger particle size, broader size distribution, and AIQ in SNCDs. These results showed that the SNCDs, which exhibited weak fluorescence in the solid state or greatly quenched fluorescence owing to aggregation, could not be used as fluorescent agents for detecting bacteria in real-time, in contrast to the SFCDs. The multicolored fluorescence emission of SFCDs was beneficial for the selection of the observation channel. The resulting LSCM images showed that 1 min-SFCD-SSM-stained bacteria had tunable fluorescence characteristics similar to those of the SFCD powder, which emitted blue fluorescence under 405 nm light excitation (blue channel) and green fluorescence under 488 nm light excitation (green channel). However, SYTO9-stained bacteria showed only

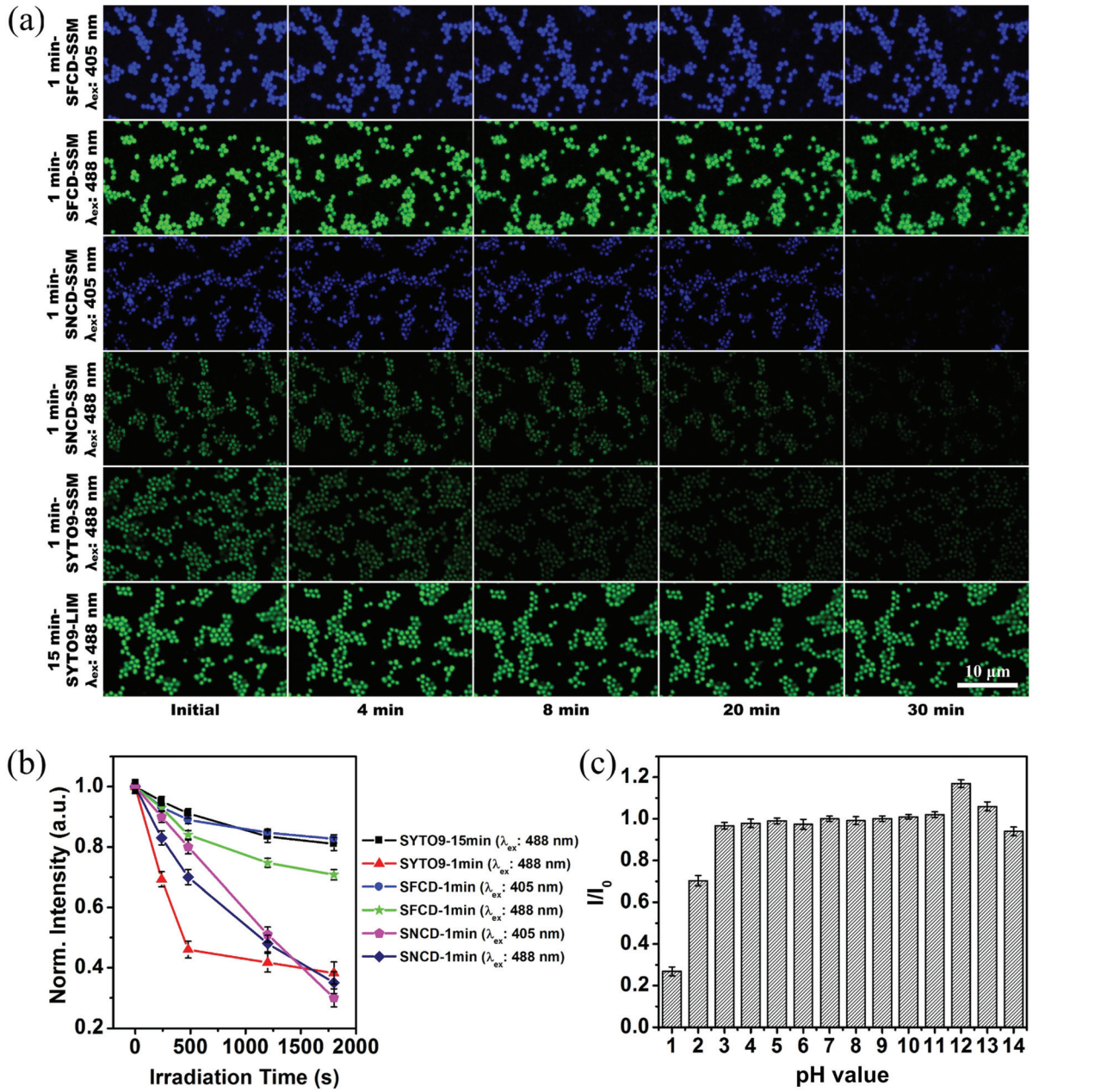


**Fig. 3** (a) Fluorescence images under LSCM of *Staphylococcus aureus* bacteria and fluorescent stability of SFCD, SNCD and SYTO9 samples, denoted as 1 min-SFCD-SSM, 1 min-SNCD-SSM, 1 min-SYTO9-SSM, and 15 min-SYTO9-LIM for 30 min continuous irradiation with a laser beam. (b) Time-dependent intensity decay curves of 1 min-SFCD-SSM, 1 min-SNCD-SSM, 1 min-SYTO9-SSM, and 15 min-SYTO9-LIM samples. (c) pH-Dependent PL intensities of the SFCD solution. "$I$" is the PL intensity, "$I_0$" is the PL intensity when the solution pH is 7.

green fluorescence due to excitation wavelength-independent PL behaviors. The brightness of strong blue and green fluorescence from 1 min-SFCD-SSM-stained bacteria was similar to that of 15 min-SYTO9-LIM-stained bacteria, but brighter than that of 1 min-SYTO9-SSM-stained bacteria (the same rapid staining procedure that was used for the SFCDs). After continuous irradiation with a laser beam for 30 min, no obvious attenuation of intensity was observed in the 1 min-SFCD-SSM-stained bacteria and 15 min-SYTO9-LIM-stained bacteria; however, the maximum fluorescence intensity was reduced to 40% of the initial intensity for the 1 min-SYTO9-SSM-stained samples and to 30% of the initial intensity for the 1 min-SNCD-SSM-stained samples (Fig. 3b). Moreover, in both the blue and green channels, the changes in fluorescence intensity were minimal for the 1 min-SFCD-SSM-stained *Staphylococcus aureus* after lucifuge storage for 8 days (Fig. S6†). In addition, SFCDs had a broad range of stabilities in solutions of different pH values ranging from 3 to 11 (Fig. 3c), further demonstrating the strong stability of SFCDs. These results illustrated that SFCDs had excellent dyeing effects similar to those of the commercial dye SYTO9, but with a faster dyeing speed. Moreover, SFCDs had good photobleaching resistance and high stability, which may be favorable for preservation of stained specimens.

To elucidate the potential applications of SFCDs as fluorescent imaging agents for monitoring various bacteria in real-time, we investigated the ability of SFCDs to stain for various representative bacteria. Fig. 4 shows LSCM images of SFCD stained slides of three types of bacteria (Gram-positive bacteria, Gram-negative bacteria, and acid-fast bacteria), including *Bacillus anthracis* (vegetative cells), *Bacillus anthracis* (endospores), *Clostridium sporogenes* (vegetative cells and endospores), *Listeria monocytogenes*, *Enterococcus faecalis*, *Yersinia pestis*, *Vibrio cholera* O1, *Neisseria meningitidis*, *Klebsiella pneumoniae*, and *Mycobacterium smegmatis*. As depicted in Fig. 4, strong blue and green fluorescence could be observed after dropping SFCD solution on slides containing bacteria for 1 min. These high-quality images obtained from this analysis implied that the staining coverage was sufficient in the cytoplasmic area of bacteria despite aggregation of SFCDs. The bacteria shown in Fig. 4 are usually difficult to stain and detect, particularly bacterial endospores and viable but non-culturable state (VBNC) bacteria, including *Bacillus anthracis* endospores, *Clostridium sporogenes* endospores, and *Yersinia pestis*, *Vibrio cholera* O1, *Listeria monocytogenes*, *Klebsiella pneumoniae*, *Enterococcus faecalis*, and *Mycobacterium smegmatis*. An endospore is a dormant, tough, non-reproductive structure produced by certain bacteria from the Firmicutes phylum and are often metabolically inert.[23] Visualizing endospores under light microscopy is difficult due to the impermeability of the endospore wall to dyes and stains from general methods. The endospore wall structure is complex and composed of exosporium, an endospore coat, an endospore cortex and a core wall. The endospore coat acts as a permeability barrier to protect the cell's DNA and vital proteins from adverse environmental conditions (excessive heating, drying, radiation, low nutrient content, *etc*.) and can also prevent dyes from entering.[24] VBNC bacteria refer to bacteria that are in a state of very low metabolic activity and do not divide, but are alive and have the ability to become culturable once resuscitated.[25] VBNC bacteria lose the capacity for growth and reproduction in standard culture medium and cannot be detected by conventional culture methods. However, VBNC bacteria are still virulent and can be considered as eliciting so-called stealth infections.[26] Once foodborne pathogens acquire the VBNC state, leakage, which causes severe public health crises and accidents, may occur.[3b,27] Therefore, effective methods for detecting VBNC bacteria are necessary for food security and human health. Our LSCM fluorescence images based on SFCD-stained

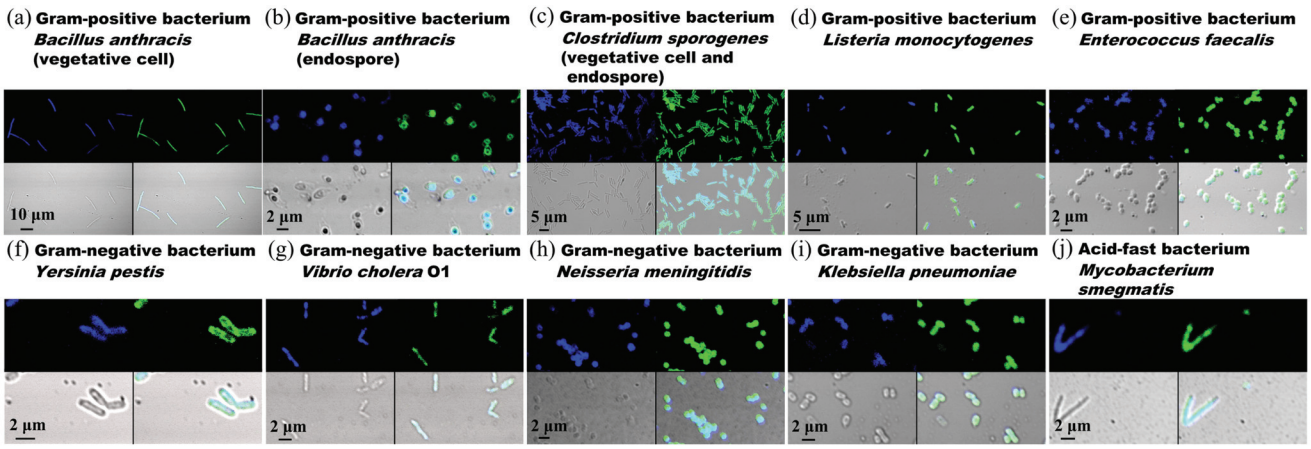


Fig. 4 Fluorescence images of SFCD-stained bacteria obtained using an LSCM. (a) *Bacillus anthracis* (vegetative cells). (b) *Bacillus anthracis* (endospores). (c) *Clostridium sporogenes* (vegetative cells and endospores). (d) *Listeria monocytogenes*. (e) *Enterococcus faecalis*. (f) *Yersinia pestis*. (g) *Vibrio cholera* O1. (h) *Neisseria meningitidis*. (i) *Klebsiella pneumoniae*. (j) *Mycobacterium smegmatis*. For (a–j), the upper left and upper right panels are blue and green fluorescence images taken with excitation wavelengths of 405 and 488 nm, respectively; the lower left panels show images of bacteria under bright field illumination; the lower right panels are overlays of the three other panels. These bacteria were all stained with SFCDs by SSM within 1 min.

 

bacteria showed that SFCDs may be used to stain all of the above-mentioned bacterial endospores and VBNC bacteria within 1 min at room temperature. In addition, another five representative bacteria, *i.e.*, *Staphylococcus aureus*, *Streptococcus pneumoniae*, *Bacillus subtilis* (vegetative cells and endospores), *Pseudomonas aeruginosa*, and *Escherichia coli*, were stained with SFCDs by SSM, as shown in Fig. S7.† These bacteria used in our work were chosen from all bacteria as some of the most representative species. These results suggested that SFCDs could permeate and diffuse rapidly in all species of bacteria, indicating that SFCDs may be promising agents for application in the detection and enumeration of total bacteria in real-time. We compared our findings with 12 previous studies, as shown in Table S4.† The present work demonstrated the best performance in bacteria staining utilizing SFCDs, which could be prepared quickly and could stain 14 representative bacteria, including some representative pathogenic bacteria, within just 1 min. The SFCDs turned out to be promising bioimaging agents, and can take on even larger roles in real-time monitoring of TBC when combined with automated practical solid flow cytometry.[28] The observed ultra-fast staining could be attributed to electrostatic repulsion, the small size of the SFCDs, and the high concentration of SFCDs, allowing maintenance of an effective concentration gradient in bacterial cells *in vitro* and *in vivo* of bacteria. The zeta potentials of SFCDs and SNCDs were evaluated to validate the surface charge; the zeta potentials of the SFCDs and SNCDs were −0.24 and −0.01 mV, respectively. Previous studies have demonstrated that nanoparticles with a high negative charge are more readily enriched in bio-cells than nanoparticles with a low negative charge, resulting in rapid permeation into the cytoplasm.[29] Considering the ultra-fast staining of bacterial endospores and VBNC bacteria with very low metabolic activity, perhaps the most probable mechanism is that SFCDs, which had an average size of 2.3 nm, may permeate and aggregate inside cells without requiring endocytosis,[30] allowing them to exhibit weak physical interactions with intracellular proteins through electrostatic interactions. In order to further confirm the superior staining of SFCDs using different staining methods, *Bacillus anthracis* endospores were also stained with SFCDs for 1 min using the LIM method. Similarities in the images of *Bacillus anthracis* endospores produced by 1 min-SFCD-SSM and 1 min-SFCD-LIM staining (Fig. S8†) demonstrated that SFCDs were also effective for staining using the LIM method. Furthermore, the bright fluorescence images of intact bacterial cells contrasted with images of unstained cell debris (Fig. S9†), indicating that SFCDs were not prone to fluorescence interference from binding with other biological impurities. Thus, staining by SFCDs exhibited high efficiency, brightness, and wide applicability. Optimizations of the concentrations of SFCDs are shown in Fig. S10 and S11,† and the PLE and PL spectra of the SFCD solution are shown in Fig. S12.†

The biocompatibility and toxicity of SFCDs were evaluated by the plate counting method (Fig. 5). The data for plate counting in Fig. 5a indicated that there were no significant differences ($p = 0.37 > 0.05$, *t*-test) in cell viability between the initial and stained bacteria (incubated for 1 min; 307 ± 5 and 317 ± 17 live bacteria, respectively). Moreover, as shown in Fig. 5b, there were no significant differences ($p = 0.65 > 0.05$, *t*-test) between the initial and stained bacteria, even after incubation for 40 min. Layer scanning was carried out in HeLa cells using the 1 min-SFCD-SSM staining method to demonstrate the low genotoxicity of the SFCDs (Fig. S13†). In cell genetics, genotoxicity describes the possibility that synthetic dyes damage the genetic information encoded within nucleic acids in a cell, causing mutations that may lead to carcinogenesis and teratogenesis.[31] The unstained nuclei of HeLa cells provided evidence of the lack of nucleic acid binding-based teratogenic and carcinogenic effects. Layer scanning and higher-magnification images of an *Escherichia coli* cell based on 1 min-SFCD-SSM staining also confirmed the mechanism observed in our analysis of HeLa cells (Fig. S14 and S15†). The results showed that the SFCDs were distributed evenly throughout the *E. coli* cell but were excluded from the nucleoids, as observed in the HeLa cell. A three-dimensional video of an *E. coli* cell (ESI Video 1†) showed that the nucleoid area of the *E. coli* cell was not stained. These results demon-

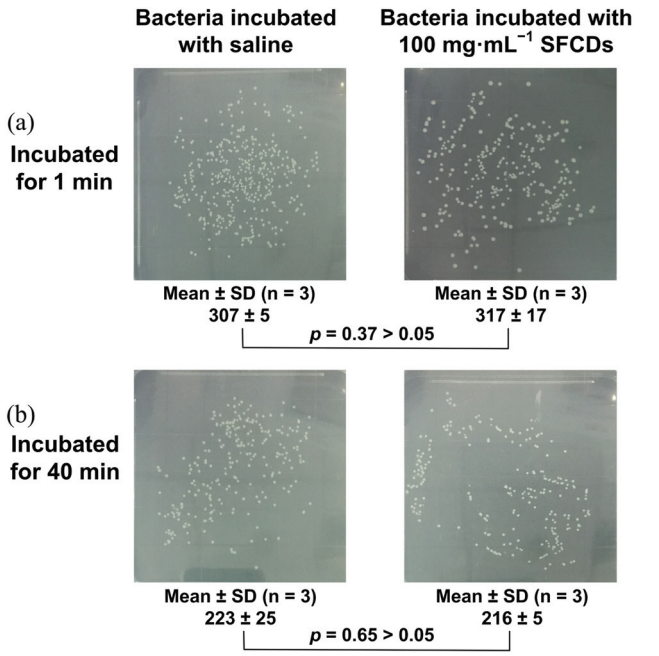


**Fig. 5** The biocompatibility and toxicity of SFCDs were evaluated by the plate counting method. (a) The suspension of $10^8$ cfu mL$^{-1}$ live *E. coli* was divided into six parts; three were stained with 100 mg mL$^{-1}$ SFCDs for 1 min (stained bacteria), and three were incubated with saline for 1 min (initial bacteria). (b) The suspension of $10^8$ cfu mL$^{-1}$ live *E. coli* was divided into six parts; three were stained with 100 mg mL$^{-1}$ SFCDs for 40 min (stained bacteria), and three were incubated with saline for 40 min (initial bacteria). (a) and (b) were conducted independently. The six bacterial suspensions were collected by centrifugation and washing twice with saline. Then samples were then diluted to about $10^3$ cfu mL$^{-1}$, and 200 μL was added to each plate for counting. The bacteria were grown in LB medium at 37 °C for 12 h prior to counting.

strated that SFCDs were promising low-toxicity fluorescence staining agents for bioimaging applications.

## Conclusions

In this paper, we fabricated SFCDs without any solid matrices using a one-step microwave synthesis process with precise control of synthesis conditions. The as-prepared SFCD powder exhibited a maximum PL quantum yield of 40% with self-quenching-resistance and was used as a highly efficient imaging agent for rapid staining of 14 representative bacteria species, including Gram-negative, Gram-positive, and acid-fast bacteria (such as *Bacillus anthracis* [vegetative cells and endospores], *Clostridium sporogenes* [vegetative cells and endospores], *Listeria monocytogenes*, *Bacillus subtilis* [vegetative cells and endospores], *Staphylococcus aureus*, *Streptococcus pneumoniae*, *Enterococcus faecalis*, *Neisseria meningitidis*, *Yersinia pestis*, *Pseudomonas aeruginosa*, *Klebsiella pneumoniae*, *Escherichia coli*, *Vibrio cholera* O1, and *Mycobacterium smegmatis*), by ultra-fast staining within 1 min without any incubation, and the fluorescence images were bright with clear contours. Moreover, excellent staining quality, superior resistance to photobleaching, high stability in solutions of different pH values, and low toxicity were also demonstrated. Thus, the SFCDs reported in this study may be promising low-toxicity fluorescence bioimaging agents with applications in the real-time monitoring of TBCs when combined with automated practical solid flow cytometry. These SFCDs could have significant applications in the fields of microbiology, environmental protection, customs examination, clinical diagnostics, public health, food safety, and biosafety.

## Conflict of interest

The authors declare no competing financial interest.

## Acknowledgements

This work was funded by the Innovation Program of Chinese Academy of Sciences (CAS), National Natural Science Foundation of China (no. 51503196), National High Technology Research and Development Program of China (no. 2013AA032205), the Major National Science and Technology Programs of China (no. 2011ZX10004 and 2012ZX1004801), Jilin Province Science and Technology Research Project no. 20140520119JH and 20150101039JC, and project supported by State Key Laboratory of Luminescence and Applications.

## References

1 (*a*) J. Liu, Y. Liu, N. Liu, Y. Han, X. Zhang, H. Huang, Y. Lifshitz, S.-T. Lee, J. Zhong and Z. Kang, *Science*, 2015, **347**, 970; (*b*) S. Liu, J. Tian, L. Wang, Y. Zhang, X. Qin, Y. Luo, A. M. Asiri, A. Al-Youbi and X. Sun, *Adv. Mater.*, 2012, **24**, 2037; (*c*) W. F. Zhang, H. Zhu, S. F. Yu and H. Y. Yang, *Adv. Mater.*, 2012, **24**, 2263; (*d*) X. Zhang, Y. Zhang, Y. Wang, S. Kalytchuk, S. V. Kershaw, Y. Wang, P. Wang, T. Zhang, Y. Zhao, H. Zhang, T. Cui, Y. Wang, J. Zhao, W. W. Yu and A. L. Rogach, *ACS Nano*, 2013, **7**, 11234; (*e*) Y. Li, Y. Hu, Y. Zhao, G. Shi, L. Deng, Y. Hou and L. Qu, *Adv. Mater.*, 2011, **23**, 776; (*f*) Y.-P. Sun, B. Zhou, Y. Lin, W. Wang, K. A. S. Fernando, P. Pathak, M. J. Meziani, B. A. Harruff, X. Wang, H. Wang, P. G. Luo, H. Yang, M. E. Kose, B. Chen, L. M. Veca and S.-Y. Xie, *J. Am. Chem. Soc.*, 2006, **128**, 7756; (*g*) D.-Y. Guo, C.-X. Shan, S.-N. Qu and D.-Z. Shen, *Sci. Rep.*, 2014, **4**, 7469; (*h*) W. Shi, X. Li and H. Ma, *Angew. Chem., Int. Ed.*, 2012, **51**, 6432; (*i*) D. Qu, M. Zheng, J. Li, Z. Xie and Z. Sun, *Light: Sci. Appl.*, 2015, **4**, e364; (*j*) A. Galeone, G. Vecchio, M. A. Malvindi, V. Brunetti, R. Cingolani and P. P. Pompa, *Nanoscale*, 2012, **4**, 6401; (*k*) C. Ding, A. Zhu and Y. Tian, *Acc. Chem. Res.*, 2013, **47**, 20.

2 (*a*) Y. Chen, M. Zheng, Y. Xiao, H. Dong, H. Zhang, J. Zhuang, H. Hu, B. Lei and Y. Liu, *Adv. Mater.*, 2016, **28**, 312; (*b*) S. Qu, X. Wang, Q. Lu, X. Liu and L. Wang, *Angew. Chem., Int. Ed.*, 2012, **51**, 12215.

3 (*a*) M. R. Taylor, *N. Engl. J. Med.*, 2011, **365**, e18; (*b*) R. G. Hoff, D. E. Newman and J. L. Staneck, *J. Clin. Microbiol.*, 1985, **21**, 513; (*c*) C. T. Muller, I. Uckay and J. Y. Beaulieu, *J. Plast. Reconstr. Aesthet. Surg.*, 2014, **67**, 1451.

4 (*a*) T. K. Mandal and N. Parvin, *J. Biomed. Nanotechnol.*, 2011, **7**, 846; (*b*) V. N. Mehta, S. Jha and S. K. Kailasa, *Mater. Sci. Eng., C*, 2014, **38**, 20; (*c*) S. Chandra, P. Patra, S. H. Pathan, S. Roy, S. Mitra, A. Layek, R. Bhar, P. Pramanik and A. Goswami, *J. Mater. Chem. B*, 2013, **1**, 2375; (*d*) H. Ding, F. Du, P. Liu, Z. Chen and J. Shen, *ACS Appl. Mater. Interfaces*, 2015, **7**, 6889; (*e*) D. Zhong, Y. Zhuo, Y. Feng and X. Yang, *Biosens. Bioelectron.*, 2015, **74**, 546.

5 D. Pan, J. Zhang, Z. Li, Z. Zhang, L. Guo and M. Wu, *J. Mater. Chem.*, 2011, **21**, 3565.

6 X. Li, S. Zhang, S. A. Kulinich, Y. Liu and H. Zeng, *Sci. Rep.*, 2014, **4**, 4976.

7 Y. Deng, D. Zhao, X. Chen, F. Wang, H. Song and D. Shen, *Chem. Commun.*, 2013, **49**, 5751.

8 Y. Deng, X. Chen, F. Wang, X. Zhang, D. Zhao and D. Shen, *Nanoscale*, 2014, **6**, 10388.

9 D. Mosconi, D. Mazzier, S. Silvestrini, A. Privitera, C. Marega, L. Franco and A. Moretto, *ACS Nano*, 2015, **9**, 4156.

10 M. Sun, S. Qu, Z. Hao, W. Ji, P. Jing, H. Zhang, L. Zhang, J. Zhao and D. Shen, *Nanoscale*, 2014, **6**, 13076.

11 (*a*) Z. Xie, F. Wang and C. Liu, *Adv. Mater.*, 2012, **24**, 1716; (*b*) F. Wang, Z. Xie, H. Zhang, C. Liu and Y. Zhang, *Adv. Funct. Mater.*, 2011, **21**, 1027.

12 S.-T. Yang, L. Cao, P. G. Luo, F. Lu, X. Wang, H. Wang, M. J. Meziani, Y. Liu, G. Qi and Y.-P. Sun, *J. Am. Chem. Soc.*, 2009, **131**, 11308.

 

13 M. Xu, G. He, Z. Li, F. He, F. Gao, Y. Su, L. Zhang, Z. Yang and Y. Zhang, *Nanoscale*, 2014, **6**, 10307.
14 D. P. Breakwell, R. B. Moyes and J. Reynolds, *Curr. Protoc. Microbiol.*, 2009, **15**, A.3I.1.
15 (*a*) I. W. Devoe and J. E. Gilchrist, *Infect. Immun.*, 1974, **10**, 872; (*b*) G. Cortés, N. Borrell, B. D. Astorza, C. Gómez, J. Sauleda and S. Alberti, *Infect. Immun.*, 2002, **70**, 2583.
16 N. Fethke and R. J. Anderson, *Am. Rev. Tuberc.*, 1948, **57**, 294.
17 Y. Dong, H. Pang, H. B. Yang, C. Guo, J. Shao, Y. Chi, C. M. Li and T. Yu, *Angew. Chem., Int. Ed.*, 2013, **52**, 7800.
18 (*a*) Z. Yang, Z. Yao, G. Li, G. Fang, H. Nie, Z. Liu, X. Zhou, X. Chen and S. Huang, *ACS Nano*, 2011, **6**, 205; (*b*) M.-S. Park, J.-S. Yu, K. J. Kim, G. Jeong, J.-H. Kim, Y.-N. Jo, U. Hwang, S. Kang, T. Woo and Y.-J. Kim, *Phys. Chem. Chem. Phys.*, 2012, **14**, 6796; (*c*) S. Yang, L. Zhi, K. Tang, X. Feng, J. Maier and K. Müllen, *Adv. Funct. Mater.*, 2012, **22**, 3634.
19 (*a*) D. Qu, M. Zheng, L. Zhang, H. Zhao, Z. Xie, X. Jing, R. E. Haddad, H. Fan and Z. Sun, *Sci. Rep.*, 2014, **4**, 5294; (*b*) Z.-H. Sheng, L. Shao, J.-J. Chen, W.-J. Bao, F.-B. Wang and X.-H. Xia, *ACS Nano*, 2011, **5**, 4350.
20 J. Sun, S. Yang, Z. Wang, H. Shen, T. Xu, L. Sun, H. Li, W. Chen, X. Jiang, G. Ding, Z. Kang, X. Xie and M. Jiang, *Part. Part. Syst. Charact.*, 2015, **32**, 434.
21 (*a*) K. P. Loh, Q. Bao, G. Eda and M. Chhowalla, *Nat. Chem.*, 2010, **2**, 1015; (*b*) S. K. Cushing, M. Li, F. Huang and N. Wu, *ACS Nano*, 2013, **8**, 1002.
22 (*a*) Y. Zhang, X. Liu, Y. Fan, X. Guo, L. Zhou, Y. Lv and J. Lin, *Nanoscale*, 2016, **8**, 15281; (*b*) Y. Zhang, Y. Hu, J. Lin, Y. Fan, Y. Li, Y. Lv and X. Liu, *ACS Appl. Mater. Interfaces*, 2016, **8**, 25454.
23 (*a*) P. R. Murray, E. J. Baron, M. A. Pfaller, F. C. Tenover and R. H. Yolken, *Manual of Clinical Microbiology*, ASM, Washington, D.C., 7th edn, 2003; (*b*) C. M. Hogan, Bacteria, in *Encyclopedia of Earth*, ed. S. Draggan and C. J. Cleveland, National Council for Science and the Environment, Washington, DC, 2010.
24 M. D. Lechtman, J. W. Bartholomew, A. Phillips and M. Russo, *J. Bacteriol.*, 1965, **89**, 848.
25 J. D. Oliver, *J. Microbiol.*, 2005, **43**, 93.
26 H.-S. Xu, N. Roberts, F. L. Singleton, R. W. Attwell, D. J. Grimes and R. R. Colwell, *Microb. Ecol.*, 1982, **8**, 313.
27 (*a*) A. Nasim and T. Brychcy, *Mutat. Res.*, 1979, **65**, 261; (*b*) N. A. Littlefield, B. N. Blackwell, C. C. Hewitt and D. W. Gaylor, *Fundam. Appl. Toxicol.*, 1985, **5**, 902.
28 (*a*) F. D'Souza, A. Bruin, R. Biersteker, G. Donnelly, J. Klijnstra, C. Rentrop and P. Willemsen, *J. Ind. Microbiol. Biotechnol.*, 2010, **37**, 363; (*b*) Mu. Yu, L. Wu, T. Huang, S. Wang and X. Yan, *Anal. Methods*, 2015, **7**, 3072.
29 (*a*) A. Feswick, R. J. Griffitt, K. Siebein and D. S. Barber, *Aquat. Toxicol.*, 2013, **130**, 210; (*b*) K. T. Thurn, E. Brown, A. Wu, S. Vogt, B. Lai, J. Maser, T. Paunesku and G. E. Woloschak, *Nanoscale Res. Lett.*, 2007, **2**, 430; (*c*) B. A. Manhat, A. L. Brown, L. A. Black, J. B. A. Ross, K. Fichter, T. Vu, E. Richman and A. M. Goforth, *Chem. Mater.*, 2011, **23**, 2407.
30 S. Y. Lim, W. Shen and Z. Gao, *Chem. Soc. Rev.*, 2015, **44**, 362.
31 (*a*) L. R. Ferguson and W. A. Denny, *Mutat. Res.*, 1991, **258**, 123; (*b*) D. Bassi, F. Cappa and P. S. Cocconcelli, *Food Microbiol.*, 2013, **33**, 11; (*c*) I. Al-Khatib, R. Giacaman, A. Husseini, A. Ramlawi, I. Atiyya and I. Salem, *Int. J. Environ. Health Res.*, 2004, **14**, 443.